Legal Medicine 49 (2021) 101836

Contents lists available at ScienceDirect

Legal Medicine

journal homepage: www.elsevier.com/locate/legalmed

Determining the effect of water temperature on the T1 and T2 relaxation times of the lung tissue at 9.4 T MRI: A drowning mouse model

Saki Kodama [a,*], Junichi Hata [b,d], Yoshimasa Kanawaku [c], Hiroshi Nakagawa [a], Hinako Oshiro [d], Erisha Saiki [e], Hirotaka Okano J. [b], Kimiharu Iwadate [a]

[a] Department of Forensic Medicine, The Jikei University School of Medicine, Tokyo, Japan
[b] Division of Regenerative Medicine, The Jikei University School of Medicine, Tokyo, Japan
[c] Department of Legal Medicine, Nippon Medical School, Tokyo, Japan
[d] RIKEN Center for Brain Science, Saitama, Japan
[e] Laboratory Animal Facilities, The Jikei University School of Medicine, Tokyo, Japan

ARTICLE INFO

Keywords:
Lung tissue
Pulmonary
T1 relaxation time
T2 relaxation time
Postmortem MRI
Drowning
Forensic

ABSTRACT

Japanese individuals have a unique culture of soaking in a bathtub, and forensic pathologists have experienced fatal cases due to drowning. However, T1 and T2 relaxation times of a drowning lung are poorly documented.

In the present study, we investigated the relationship between drowning water temperature and T1 and T2 relaxation times of drowning lung tissues at 9.4 T MRI (Bruker, BioSpec94/20USR). The mice used as animal drowning models were directly submerged in freshwater. Water temperature was set to 8 °C–10 °C (cold), 20 °C–22 °C (normal), 30 °C, and 45 °C. The regions of interest (ROIs) on the axial section of the third slice were set at the central and peripheral areas of each—the left and the right—lung. T1 relaxation times measured immediately after death differed by the presence or absence of soaking water, except in case of cold water temperature. In the drowning groups, T1 relaxation time showed a linear dependency on water temperature. By contrast, T2 relaxation time was almost constant regardless of the presence of drowning under the same temperature condition; when compared in the lung areas of the same individuals, the times were uniformly reduced in drowning models. To minimize the effects of hypostasis and decomposition, we performed measurements immediately after death and were able to determine the noticeable difference in drowning water temperature. These results may be useful for qualitative assessments of a drowning lung and may serve as a basis when imaging the human body during forensic autopsy cases.

1. Introduction

Recently, nuclear magnetic resonance (NMR) relaxation measurements have facilitated the visualization of the changes in the lung tissues caused by gravitation [1], respiration [2], lung injury [3], or clinical pulmonary disease [4,5]. The Bloembergen–Purcell–Pound theory describes that changes in T1 and T2 values are primarily related to changes in temperature [6]. To date, the NMR theory has shown that T1 relaxation time exhibits a simple linear relationship with the temperature, that T2 temperature dependence is relatively small [7,8], and that T2 relaxation time depends on tissue types [9]. Furthermore, the theory has been applied in postmortem magnetic resonance imaging (MRI) study. Previous studies have reported that T1 relaxation time exhibits a linear dependency on the temperature in the human brain at 3 T [10] and that a reduction in body temperature after death causes changes in T1 and T2 values in the human liver at 1.5 T [11]. Pulmonary T1 relaxation in vivo depends on respiratory factors; sex and age [12]; spatial variation caused by gravitational effects; slice positioning; and ROI selection [13]. However, the effect of the temperature of water aspirated immediately before drowning on the lung tissue during a postmortem MRI at 9.4 T

Abbreviations: NMR, nuclear magnetic resonance; MRI, magnetic resonance imaging; TE, echo time; ROI, region of interest' Control, non–drowning sudden death model made by cervical dislocation; Cold, cold water temperature drowning model; Normal, normal water temperature drowning model; Warm, lukewarm water temperature drowning model; Hot, hot water temperature drowning model.

* Corresponding author at: The Jikei University School of Medicine, Department of Forensic medicine, Nishi-Shimbashi, Minato-ku, Tokyo, JP 105-8461, Japan.
E-mail addresses: skodama@jikei.ac.jp (S. Kodama), J.Hata@jikei.ac.jp (J. Hata), ykanawaku@nms.ac.jp (Y. Kanawaku), nakanakahiro@jikei.ac.jp (H. Nakagawa), hinako.oshiro@riken.jp (H. Oshiro), erisha@jikei.ac.jp (E. Saiki), hjokano@jikei.ac.jp (H. Okano J.), iwadate@jikei.ac.jp (K. Iwadate).

https://doi.org/10.1016/j.legalmed.2020.101836
Received 8 July 2020; Received in revised form 21 November 2020; Accepted 29 December 2020
Available online 4 January 2021

remains unclear.

Forensic pathologists have experienced several fatal cases due to drowning, with drowning becoming one of the most common causes of death among the Japanese population. Particularly, Japanese individuals have a unique culture of soaking in a bathtub; hence, "bathtub drowning" is common in this population [14,15], and Japan has the highest drowning mortality among the countries of the Organization for Economic Co-operation and Development [16]. For drowning victims, the temperature of the aspirated water is a critical component of postmortem forensic investigation and is particularly important when MRI assessment is used to classify drowning as the cause of death. In Japan, several individuals indulge in the cultural habit of soaking in a bathtub that incorporates a wide range of water temperatures. Accordingly, changes in lung tissues caused by water aspiration into the airway can vary based on the temperature of the aspirated water. In this study, we provide basic T1 and T2 values of drowning lung tissues at a various water temperatures.

Forensic pathologists have focused on the type of water (fresh or saltwater) [17–19] and have reported experiences of drowning lung images on postmortem computed tomography [20,21] and pathological analysis [22]. By contrast, the T1 and T2 relaxation times of a drowning lung are poorly documented, and the ways in which the temperature of inhaled water affects drowning lung tissues remain to be elucidated. In the present study, we aimed to measure the T1 and T2 relaxation times of the lung tissue in a drowning mouse model at 9.4 T, focusing on water temperature during drowning, which was associated with the changes in lung relaxometry. We simulated the drowning taking into consideration that the water content of the lung would continue to increase. By changing only the water temperature of the aspirated water, we hypothesized that there was a relationship between pulmonary T1 relaxation and temperature the water aspirated immediately before death.

The lung parenchyma has physiological characteristics different from that of the brain and liver. The two most important properties of the lung tissue in pulmonary MRI are as follows: the low density and the susceptibility differences between the tissue and air. In healthy human lungs, the tissue density is 0.1 g/cm^3, which is approximately 10-fold lower than that in other tissues [23]. According to the theory MRI signal formation, which is directly proportional to the tissue proton density, pulmonary MRI signal is approximately 10 times weaker than that of adjacent tissues. Therefore, we focused on the condition of the drowning lung caused by the inflow of water into the alveoli. By forcibly creating a state with a high proton density, a pulmonary MRI would be possible and easier. In our experiment, we used a high-field 9.4 T MRI system and powerful gradient systems to adapt to pulmonary MRI. Here, we aimed to examine the T1 and T2 relaxation times of the lung tissues in a drowning mouse model at 9.4 T.

2. Materials and methods

2.1. Animals, anesthesia, and experimental drowning model

All procedures were reviewed and approved by the Institutional Animal Care and Use Committee of the University (No. 2018-058C1) and conformed to the Guidelines for the Proper Conduct of Animal Experiments of the Science Council of Japan (2006). We obtained male-specific pathogen-free C57BL/6JJmsSlc mice from Sankyo Laboratories (Tokyo, Japan). Mice aged 8–12 weeks were used in the experiment, and their weight ranged from 19.2 to 25.9 g (mean: 22.9 g). The total number of mice used was 80. All mice were bred under a controlled temperature (22 °C ± 2 °C) with a 12-h light/dark cycle (lights on, 7 a.m. to 7p.m.). The humidity was controlled at 45%–65%. The mice were fed with rodent diet CE-2 from CLEA (Tokyo, Japan) and had access to water ad libitum. Three types of mixed anesthesia were administered via an intraperitoneal injection (10 μg/g body weight): 0.3 mg/kg of medetomidine, 4.0 mg/kg of midazolam, and 5.0 mg/kg of butorphanol [24].

At 15 min after anesthetic administration, all mice were confirmed to be in deep coma with the loss of pedal withdrawal reflex. At this time, their rectal temperature was measured and it ranged from 29.8 °C to 31.5 °C (mean: 30.5 °C). During the experiment, the mouse was held in a prone position and placed in a 50-mL laboratory tube with both ends cut to ensure that the mouse's nose and mouth were completely submerged in 4.5 cm deep water bath containing tap water. Under deep anesthesia, the mouse's entire body was soaked for 2 min [25]. After 2 min of drowning, the mouse was removed from the bath. All mice had already drowned at the time of removal from the bath.

All mice were classified into 5 groups (n = 10 in each group):

Group I (non–drowning sudden death model, control): mice killed by cervical dislocation unrelated to drowning;
Group II (cold water drowning model, cold): water temperature set up at 8 °C–10 °C assuming the temperature in the river during winter;
Group III (normal temperature drowning model, normal): water temperature set at 20 °C–22 °C as room temperature;
Group IV (lukewarm drowning water, warm): water temperature set at 30 °C, which was approximately the same as the rectal temperature immediately before drowning;
Group V (hot water drowning, hot): water temperature set at 45 °C, which was the same at that of a hot bath.

2.2. Postmortem temperature condition

According to the relaxation theory, the temperature is a critical modulator of T1 and T2 relaxation times. Body temperature begins to decrease immediately following death, and due to technical limitations, it is not possible to monitor rectal temperature during imaging. As an alternative method, we created a drowning mouse model (which is different from that used for imaging) under the same experimental conditions. Temperature monitoring was performed immediately after death to eliminate the effects of postmortem changes.

Each animal was dissected immediately after death to measure the lung and rectal temperatures and to sample the lung tissues. The chest of the mouse was dissected open, and the lung temperature was measured via the insertion of a probe between the lobes of the right lung. Rectal temperature was simultaneously measured. Both lungs were then sampled and weighed.

For continuous monitoring of rectal temperature, we placed each animal in a 50-mL laboratory tube and wrapped a towel around the tube to mimic a system coil. The mouse was then left in a laboratory having the same environmental conditions as the MRI room. Rectal temperature was continuously monitored at 1-min intervals for 1 h. The endpoint was set at 1 h because we assumed that this was the time required for continuous measurement of T1 and T2 relaxation times. In addition to the aforementioned technical limitations, lung and rectal temperature monitoring were not simultaneously performed as the actual measurements of T1 and T2 relaxation times because lung temperature monitoring required opening the chest of mice. It is likely that this process would cause a faster decrease in body temperature and impact the results of our experiments.

2.3. MRI protocol and setting the regions of interest

After removal from the bath, the body of all mice was quickly blotted dry. Each animal was placed in prone position in a 50-mL laboratory tube, and the T1 and T2 relaxation times of the lung tissue were measured immediately after death. Measurements were performed with the 9.4 T BioSpec 94/20 (Biospin GmbH, Ettlingen, Germany) with high-power gradient magnetic field (maximum strength: 300 mT/m) using 40 mm quadrature detection system coil. The T1 and T2 mappings were obtained from each animal. For T1 mapping, rapid acquisition with relaxation enhancement was used with the following parameters: TR = 200/320/512/819/13 ms, TE = 5.9 ms, flip angle = 90°, number of

averages (NA) = 2, and scan time = 20 min and 34 s. For T2 mapping, a multiple spin-echo sequence was used with the following parameters: TR = 3000 ms; TE = acquires 20 echo at 6.5 ms intervals, with 6.5 ms as the first echo; flip angle = 90°; NA = 2; and scan time = 6 min and 24 s. The resolution was set at 0.375 × 0.375 mm in all cases.

The coronal cross-section from the height of the tracheal bifurcation to the bottom of the lung was selected for sectioning (slice thickness: 1 mm; number of acquisitions: 6). The third slice from the bottom of the six segments was used for relaxometry because the lung field in the axial section of the level was most widely observed (Fig. 1).

After measurements of relaxation time maps, the regions of interest (ROIs) were set as a circular area measuring 2.55 mm^2 in the lung at four points: ROI1, peripheral area of the left lung; ROI2, central area of the left lung; ROI3, central area of right lung; and ROI4, peripheral area of right lung. Four ROIs were performed because the central region contained more thick blood vessels than the trachea [26]. In addition, hyperventilation and impaired expiration caused alveolar inflation accompanied by pulmonary congestion during the dynamic asphyxia of drowning [27]. Therefore, a peripheral ROI was chosen as a region that contained greater amount of lung parenchyma for evaluation. For a simple assessment of the relaxation time in the drowning lung, excluding the effect of gravitation and hypostasis, peripheral ROI was set at the same height as central ROI in the axial section. Therefore, the measurement region of lung relaxometry was determined to consider various conditions such as alveolar size, oxygen enhancement, and water and blood content.

To observe changes in the T1 and T2 relaxation times caused by drowning and water temperature in each animal, T2 relaxation time was continuously measured after the measurement of T1 relaxation time. Examples of the relaxation time course of a representative mouse from each group are shown in Fig. 1.

2.4. T1 and T2 relaxation times of water using four water temperature groups

By circulating water at each temperature around a water-filled tube, we measured T1 and T2 relaxation times of water itself using four water temperature groups employing the same MRI protocol. We hypothesized that this experiment would help demonstrate the effect of aspirated water temperature on T1 and T2 relaxation times of the lung tissue.

2.5. Statistical analysis

All statistical analyses were nonparametric and performed using R software version 3.6.2. [R Core Team (2019). R: A language and environment for statistical computing. R Foundation for Statistical Computing, Vienna, Austria. URL https://www.R-project.org/]. T1 and T2 relaxation times of the lung tissue were determined using the same ROIs. T1 and T2 values were expressed as arithmetic mean value ± standard error separately for the central and peripheral regions. First, the central and peripheral regions were compared using Wilcoxon signed-rank test ($p < 0.05$, paired, two tailed). In multiple comparison of five groups, pairwise *t*-test on R 3.6.2 was applied with p-value adjusted by Bonferroni correction ($p < 0.05$). A p-value of < 0.05 was considered statistically significant. A Spearman's rank correlation coefficient was used to assess the temperature dependence of T1 relaxation time.

3. Results

MRI was successfully performed in all mice and used to measure the T1 and T2 relaxation times of the lung tissue.

3.1. Time schedule for imaging and reduction in the postmortem body temperature (Fig. 2)

Fig. 2a shows the relationship between the lung and rectal

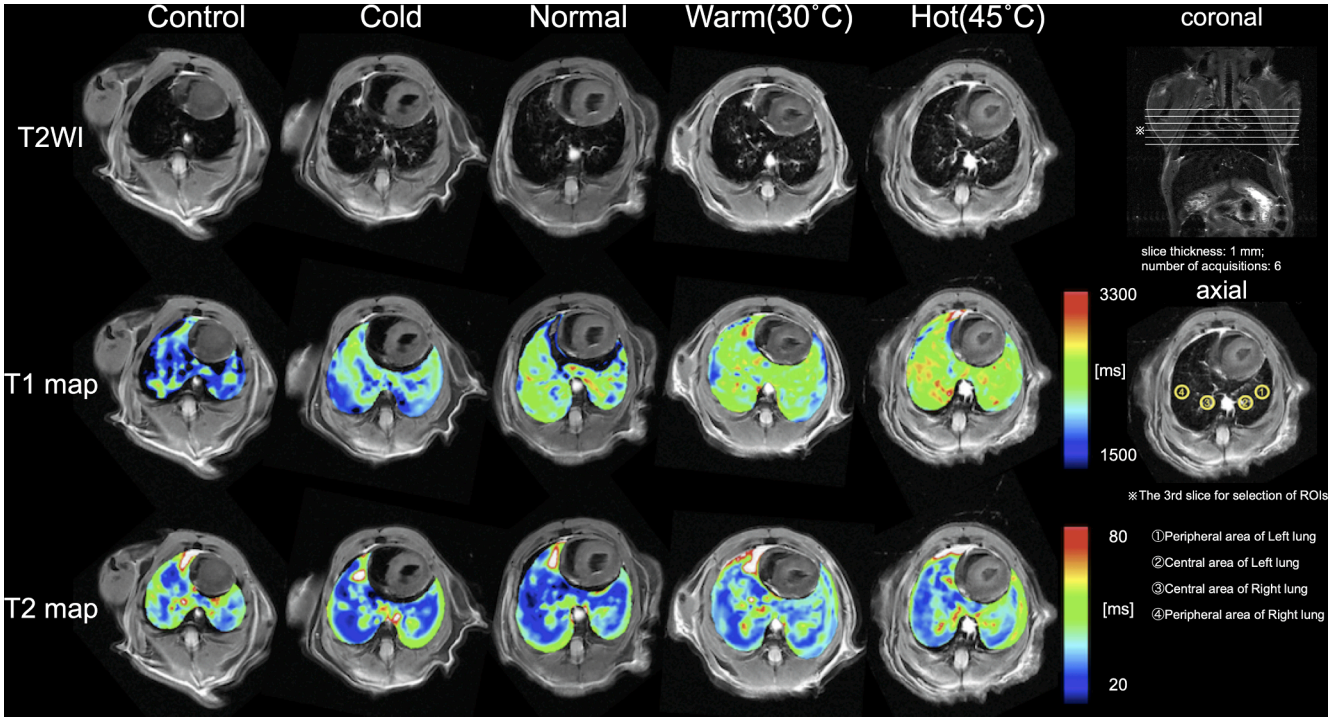

Fig. 1. Example photograph of HighResoT2Wls (top) and T1 (middle) and T2 (bottom) relaxation time maps. From the left, the cause of death of the mouse is control, cold, normal, warm, and hot water. The color maps of T1 and T2 are superimposed on the T2WI, and the color range is adjusted for contrast in the relaxation time range shown on the right bar. Coronal image (upper right) shows the number of acquisitions: 6. Axial image (middle right) shows the ROIs. In the photograph of high-resolution T2WIs, growing aspirations are shown moving into the bronchi and alveoli.

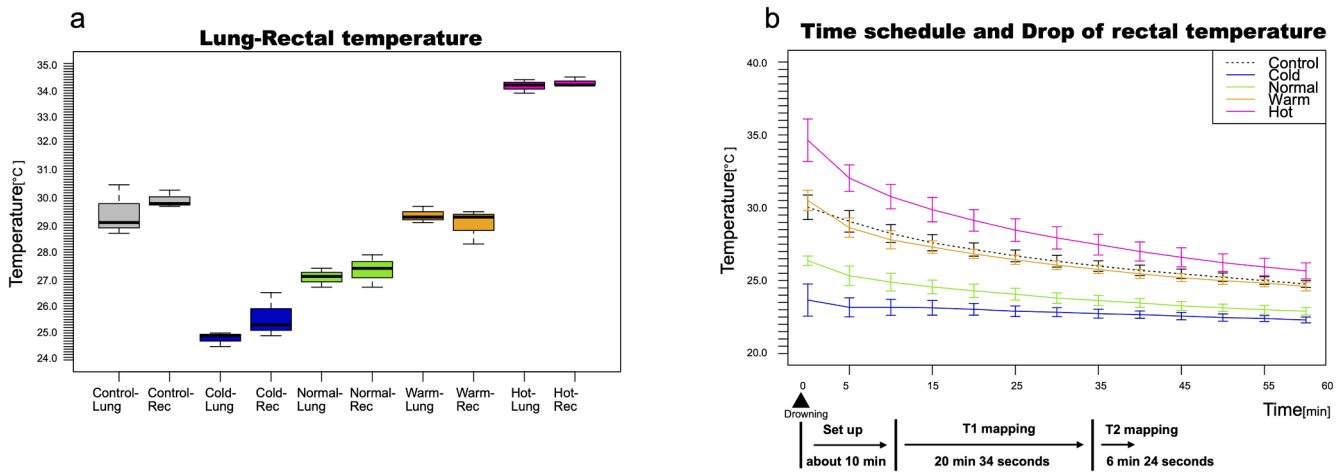

Fig. 2. Time schedule for imaging and reduction in the body temperature of dead mice. Because of the technical limitations of our device, it was impossible to measure T1 and T2 relaxation times while monitoring the lung and rectal temperatures; hence, we performed a simulation of postmortem decrease in a mouse body temperature with an individual other than the one actually used in the measurement of T1 and T2 relaxation times. Fig. 2a shows the relationship between the lung and rectal temperatures within the same individual immediately after drowning. In each group, no significant difference was observed at either temperature (paired *t*-test), although we considered that the lung temperature could be approximated by the rectal temperature. Fig. 2b shows our experimental time schedule and postmortem rectal temperature drop. All measurements were performed within the same time as this simulation, and the rectal temperature at the time of measurement is almost the same as that shown in this graph.

temperatures immediately after drowning. The mouse used for this measurement was different from that used for imaging. This result suggested that the temperature of the drowning lung can be approximated to the rectal temperature as the core body temperature. Fig. 2b shows the decrease in this rectal temperature after death and time schedule for imaging.

3.2. *T1 and T2 values of water using four water temperature groups (Table 1)*

We measured a basic value of water itself with 10 °C, 20 °C, 30 °C, and 45 °C using the same MRI protocol for lung tissues.

3.3. *Comparison of central and peripheral regions (Fig. 3)*

Initially, in control unrelated to drowning, T1 and T2 relaxation times showed no significant differences between the central and peripheral regions. Similarly, no significant differences were found on T1 relaxation time of the remaining four groups. However, in all drowning groups (cold, normal, warm, and hot), T2 relaxation time showed significant differences between the central and peripheral regions [p value $= 4.77 \times 10^{-5}$ (cold), 1.91×10^{-6} (normal), 1.91×10^{-6} (warm), and 1.91×10^{-5} (hot)] (Fig. 3). Peripheral values were evidently lower than the central values.

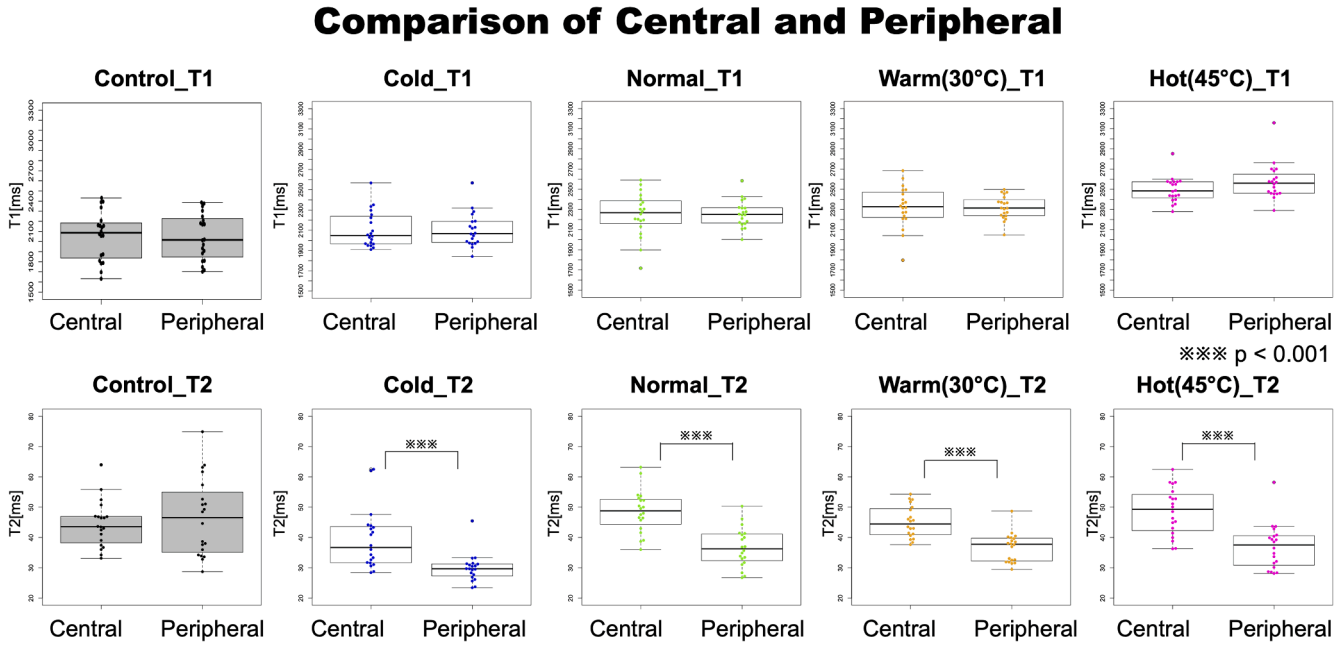

Fig. 3. MRI measurement values for each ROI in the control and four drowning groups. In T1 value, no significant differences were found. In T2 value, four drowning groups show significant differences between the central and peripheral regions ($p < 0.001$) and among each p-value. Peripheral values are clearly lower than the central values. These changes are characteristics of drowning groups. This statistical analysis was confirmed by Wilcoxon signed-rank test ($p < 0.05$, paired, two tailed).

3.4. Lung T1 in multiple comparison of five groups (Fig. 4a and b)

On comparing based on the presence or absence of drowning, on both central and peripheral regions, T1 relaxation time showed no significant differences between the control and cold groups. Particularly, the control and other drowning groups showed significant differences. On the central region, control versus normal yielded a p-value of 0.026; control versus warm, p-value of 3.6×10^{-4}; and control versus hot, p-value of 2.5×10^{-9}. On the peripheral region, control versus normal yielded a p-value of 0.0018; control versus warm, p-value of 2.3×10^{-5}; and control versus hot, p-value of 4.5×10^{-14}.

Regarding each drowning group, on the central region, cold–warm, cold–hot, and normal–hot indicated significant difference compared with control ($p = 0.0073$, 1.2×10^{-7}, and 0.0013, respectively). Other combinations showed no significant difference.

On the peripheral region, the result was similar to those on the central region but had a change in warm–hot (cold–warm, cold–hot, normal–hot, and warm–hot: $p = 0.0014$, 9.1×10^{-12}, 4.7×10^{-6}, and 4.5×10^{-4}, respectively).

3.5. Drowning water temperature dependency of lung T1 relaxation time (Fig. 5)

In drowning groups, lung T1 relaxation time showed a tendency to increase with changes in drowning water temperature (Fig. 5). On both the central and peripheral regions, T1 relaxation time showed a linear dependency on drowning water temperature. The central region of T1 demonstrated a Spearman's rank correlation of 0.63 ($p < 0.0001$), whereas the peripheral region demonstrated a correlation of 0.75 ($p < 0.0001$).

3.6. Lung T2 in multiple comparison of five groups (Fig. 6a and b)

On comparing based on whether drowned or not, unlike the change in T1 relaxation time, T2 relaxation time on the central region showed no significant differences between the control and other drowning groups. On the peripheral region, control and all drowning groups showed significant differences (control–cold, control–normal, control–warm, and control–hot: $p = 1.0 \times 10^{-8}$, 0.0012, 0.0011, and 0.0018, respectively).

Regarding each drowning group, on the central region, cold–normal and cold–hot indicated significant difference ($p = 0.0019$ and 0.0018, respectively). Other combinations had no significant differences. Additionally, on the peripheral region, there were no differences in any combination.

Importantly, in T2 relaxation time, attention should be paid to the change from central to peripheral regions in the drowning groups. As shown in Fig. 3, in control, there were no significant difference between central and peripheral T2 values. However, in all drowning groups, peripheral values were evidently lower than the central values. Therefore, in the peripheral region of T2, it was natural that there was a significant difference between the control and each drowning group.

3.7. Autopsy findings and lung weight (Table 2)

Gross autopsy showed pulmonary hyperinflation in all drowning groups; however, no gross differences were found between control and drowning groups. After autopsy, lungs from all groups were sampled and weighed and the weight of both lungs per body weight was compared. The control and all drowning groups showed significant differences ($p < 0.05$). No significant difference was found in each drowning group.

3.8. Histopathology (Fig. 7)

Histological analysis for one murine lung of each group is shown in Fig. 6. Compared with control, each drowning group showed destruction or expansion of peripheral alveolar septa; however, it was only considered as a drowning lung finding, which was not specific. Furthermore, hematoxylin–eosin staining, which is the simplest and most common staining method, did not show histological differences depending on the temperature of the drowning water.

4. Discussion

Our study aimed to evaluate the relationship between drowning water temperature and T1 and T2 relaxation times of the drowning lung tissue at 9.4 T MRI. In the case of obtaining measurements immediately after death, the values of T1 relaxation time differ by the presence or

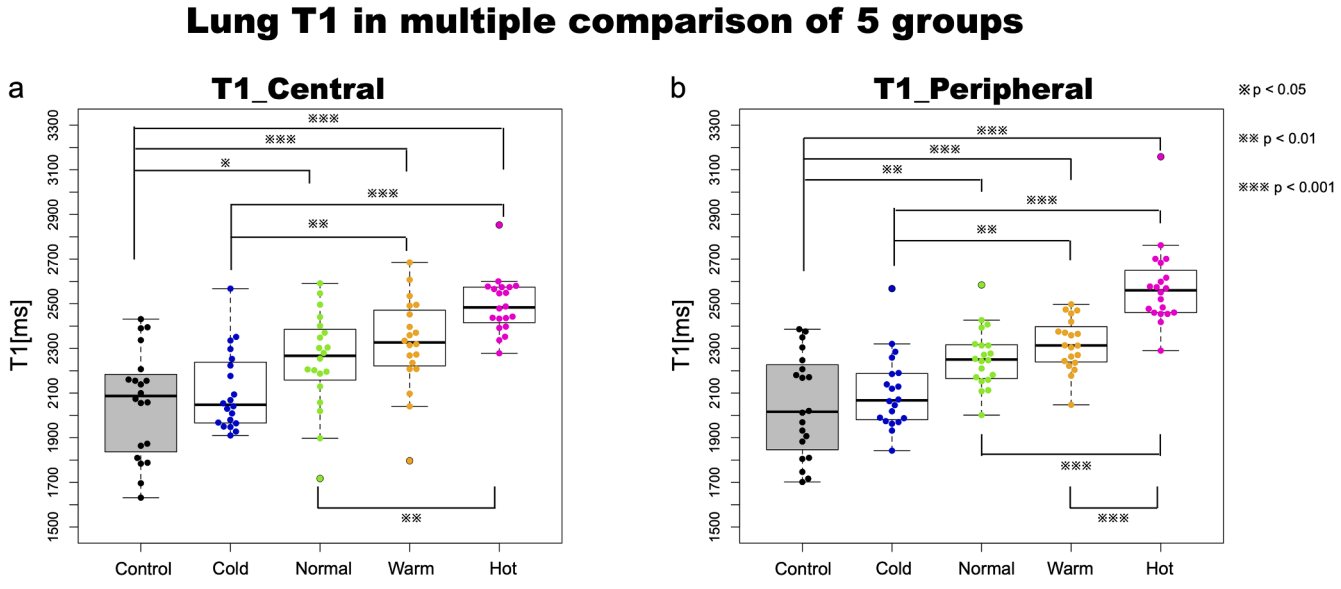

Fig. 4. Multiple comparison of lung T1 values on the central region (Fig. 4a) and peripheral region (Fig. 4b). The details of each p-value are shown in the text 3.2. On both regions, when the temperature of drowning water is low, it is not possible to distinguish the presence or absence of water suction in the T1 relaxation time. In drowning groups, the difference in the T1 relaxation time was clearer as drowning water temperature increases. Statistical analysis was confirmed by pairwise *t*-test on R 3.6.2 with p-value adjusted by Bonferroni correction ($p < 0.05$).

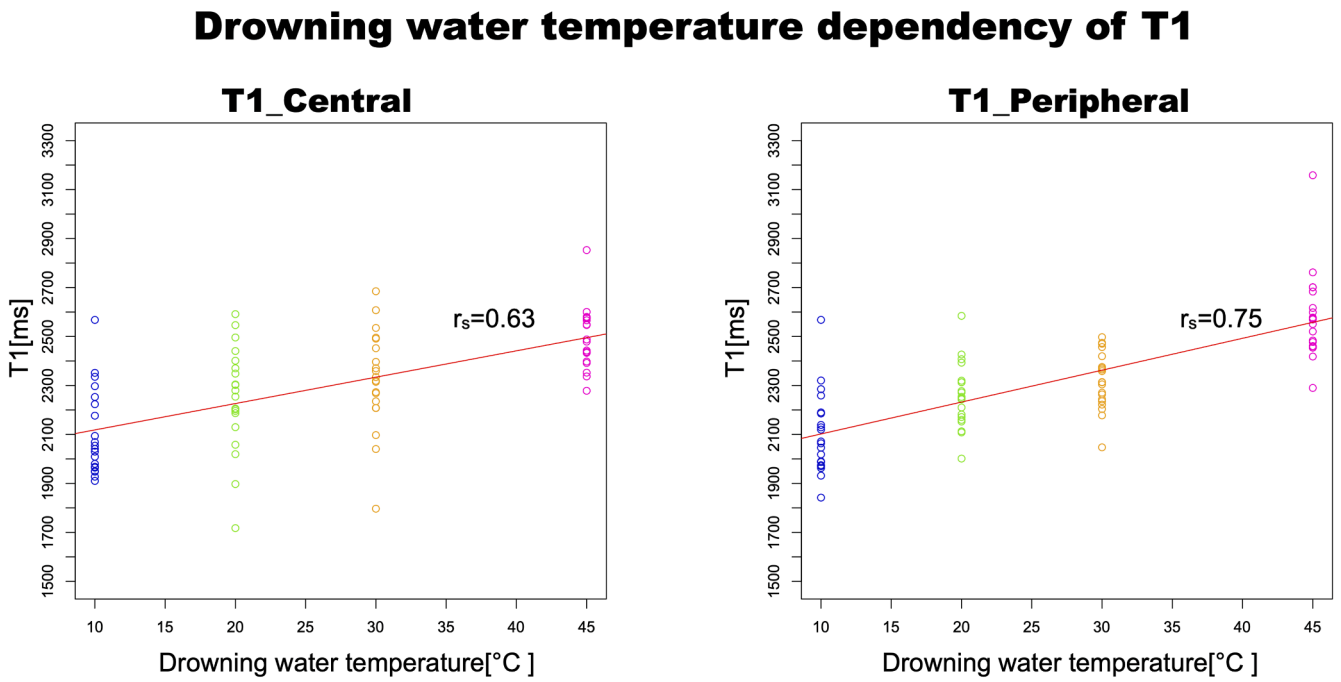

Fig. 5. Correlation diagram for the drowning water temperature dependency of lung T1 relaxation time. This result indicated that the T1 relaxation time increases as the drowning water temperature increases. This statistical analysis was confirmed by Spearman's rank correlation coefficient on R 3.6.2.

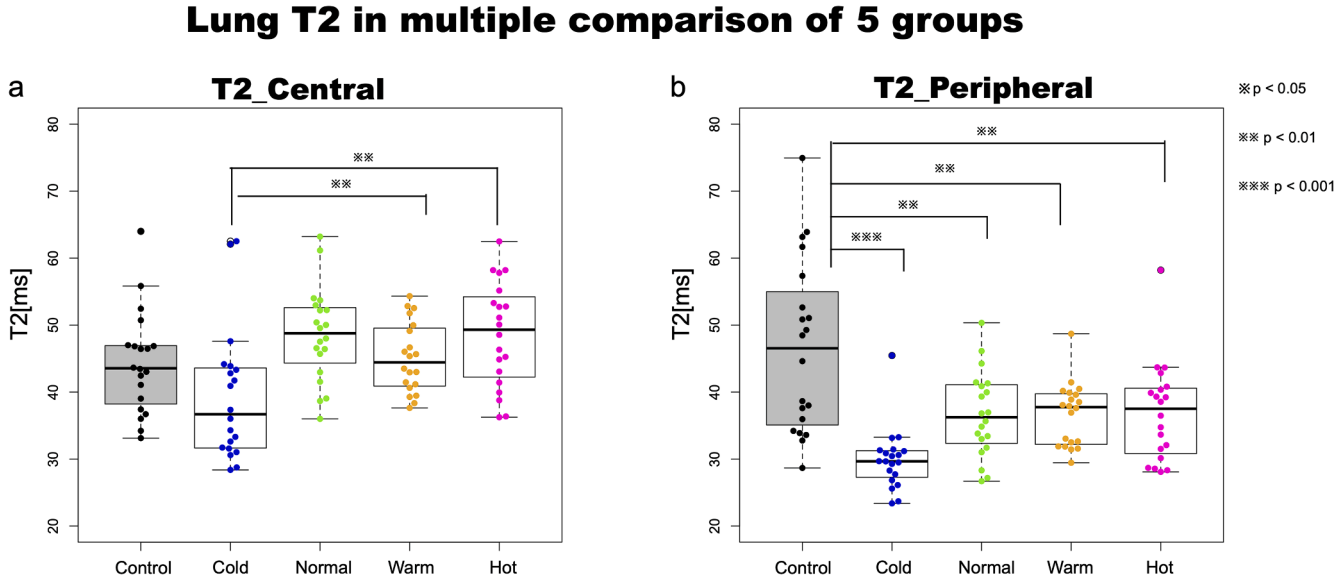

Fig. 6. Multiple comparison of lung T2 values on the central region (Fig. 5a) and the peripheral region (Fig. 5b). T2 value seemed insensitive to the drowning water temperature. However, the p-value of cold–hot on the central region was 0.0018, and the p-value of cold–hot on the peripheral region was 0.051. The other details of each p-value are shown in the text 3.3. The difference on the peripheral region between the control and drowning groups was noticeable, but the important point for evaluating T2 relaxation time was the change in the value from the central to peripheral region; hence, this statistical result is meaningless. Statistical analysis was confirmed by pairwise *t*-test on R 3.6.2 with p-value adjusted by Bonferroni correction ($p < 0.05$).

absence of soaking water, except for cold (Fig. 4a and b). Furthermore, following drowning, T1 relaxation time showed a linear dependency on water temperature (Fig. 5). By contrast, the values of T2 relaxation time were almost constant regardless of the presence of drowning under the same temperature condition; however, when the central area was compared with the peripheral area of the same individuals, they were found to be uniformly reduced in drowning models (Fig. 6a and b).

In practice, only the warm group can be an exact contrast to control. Because the temperature conditions of these two groups were almost the same, it could be evaluated only from this result whether inhaled water affected relaxation time. The difference between control and warm is clear, which may be due to the significant increase in water content caused by water aspiration. Considering the T1 value of water at each temperature (Table 1), we assessed that T1 relaxation time of the drowning lung tissue reflected on the water temperature and was sensitive to the effect of the water content.

Interestingly, in the case of cold, the T1 values were not distinguishable from control. Using gross autopsy, we confirmed that no difference in each drowning group was found in the weight of lung per body weight (Table 2). This result suggested that the drowning water

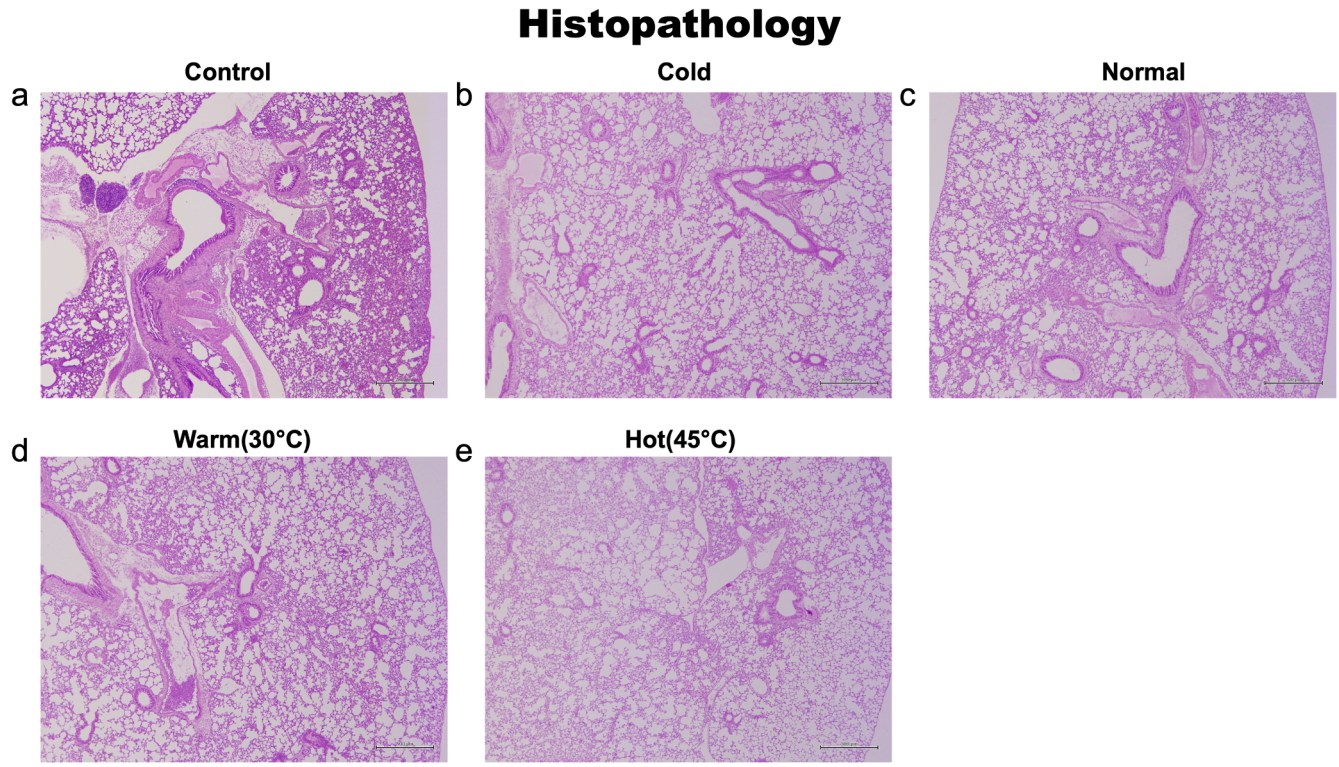

Fig. 7. Pulmonary histopathology (40× magnification, hematoxylin–eosin). Compared with control, every drowning group shows a destruction or expansion of peripheral alveolar septa, but it was only considered as a drowning lung finding, which was not specific. No characteristic findings were observed depending on the drowning temperature.

Table 1
T1 and T2 values of water with drowning temperature.

Water temperature	T1 [ms]	T2 [ms]
10 °C	1802.7 ± 74	504.8 ± 30.2
20 °C	2073.7 ± 25.5	486.9 ± 34
30 °C	2489.4 ± 24.2	454 ± 34.2
45 °C	3026.5 ± 27.1	392.7 ± 29.2

Mean ± SE

Table 2
Left and right lung weight of control and drowning groups.

	Left lung weight (mg)	Right lung weight (mg)
Control	53.5 ± 8.8	93.1 ± 3.5
Cold	151.8 ± 8.3*	194.7 ± 3.9*
Normal	137.7 ± 4.8*	169.6 ± 7.3*
Warm	137.9 ± 7*	164.7 ± 15.1*
Hot	141.5 ± 12.7*	217.7 ± 16.1*

Mean ± SE
* $p < 0.05$, compared with control group

temperature in our study did not affect the amount of water flowing into the alveoli. Therefore, we considered that a cause of the similar T1 values was not the amount of aspirated water. According to the relaxation theory, T1 relaxometry depends on the radius of the molecules, the distance between the spins of a molecule, and the viscosity of the medium [28]. Moreover, the viscosity of water is closely related to temperature, and its viscosity decreases as the temperature increases. By contrast, the NMR theory proposes that T1 in the liquids ordinarily decreases with increasing viscosity [6]; our results support the latter theory.

Indeed, in forensic practice, pre-dissection body is refrigerated after death and during transport to prevent it from decay, and these temperature conditions are likely to change the T1 relaxation time; therefore, it may not be realistic to assume that a cadaver can be imaged using MRI while it is still warm/cold from drowning. The result that the T1 value of control is indistinguishable from cold has the potential to provide useful data when matched to actual forensic conditions and warrants further study.

As for T2 relaxation time, a previous study suggested that the regional variations in pulmonary T2 relaxation time may be useful for the characterization of pulmonary diseases [29]. In our study, the T2 values of the four drowning groups were considered unique and indicated partial changes within the same individual. Control did not show this change, although it may be due to drowning. Changes in the values in the peripheral region were remarkable when compared within the same individual as well as between the control and four drowning groups. Hyperinflation via water aspiration may cause excessive airflow to the peripheral alveoli, resulting in a decrease of T2 values. Despite using the same MRI protocol, T1 and T2 values of the lung tissue were lower than that of water with the four temperature groups (Table 1), which may reflect the characteristic of air-rich lung tissue.

Regardless of the area in T1 relaxation time, in the central region of T2 relaxation time, it was easy to distinguish between hot and cold. Hot condition was a model of “bathtub drowning,” whereas cold condition simulated the situation of drowning in the river in winter. In forensic cases, we must often determine the possibility that the location of drowning is different from the place where the cadaver was found. At least in our experiments, because the measurement was obtained immediately after death to minimize the effects of decay, T1 and T2 relaxation times in the lung tissue helped to clarify the remarkable difference in drowning water temperature.

A limitation of our study is measuring T2 relaxation time after T1 relaxation time to observe the changes in the central and peripheral regions in the same individual. The imaging time itself is short because of the use of the 9.4 T MRI; however, T2 relaxation time may not be evaluated as the value immediately after drowning. Body temperature

was decreasing at the start of the T2 measurement, (Fig. 2), rendering it challenging to evaluate T2 temperature dependence. According to the NMR theory, T2 relaxation time depends on tissue types [9]; our results may follow this theory.

For an accurate forensic assessment, various factors that cause postmortem changes, such as water temperature, body position, decomposition, and autolysis with time elapsed after death, should be included in the analysis. It is essential to consider the effect of hypostasis in postmortem lung imaging. In our study, we set peripheral ROI at the same height as the central ROI in the axial section because the ROI in this animal experiment is quite small to evaluate the gravitational effect. By positioning the central and peripheral measurements at the same height, it became possible to assess the T1 and T2 relaxation time, excluding the gravitational effect.

Our results can only claim differences between non–drowning sudden death and drowning at several water temperatures at a fixed time point with respect to death. This study only provides data on the relationship between drowning water temperature and T1 and T2 relaxation time of the lung tissue immediately after death; the effect of postmortem time interval on relaxation time is not pursued here. However, as Hyodoh *et al.* reported that the lung hypostasis of postmortem CT presented differently in individual causes of death and depended on the postmortem time [30] as well as on postmortem lung MRI, the influence of time interval and the effect of hypostasis should be examined in detail in the future.

Thayyil *et al.* reported that postmortem MRI is useful for the evaluation of fetal and pediatric deaths [31,32] and that the diagnostic assessment by postmortem MRI in fetuses and children is as accurate as conventional autopsy [33,34]. Recently, they reported the degree of maceration with a whole-body fetal postmortem MRI and showed that increasing maceration was correlated with the prolongation of T2 values in the liver and lungs at 1.5 T [35]. We suppose that the changes caused by maceration are likely to be similar to those that occur in bodies drowned in water over time. Although our research will require the concept of time lapse according to actual forensic events, if we develop it further based on previous reports, it may be possible to apply the measurement of T1 and T2 relaxation times at 9.4 T MRI to better understand the tissue degeneration that occurs during postmortem changes.

5. Conclusion

Temperature dependency of T1 relaxation time was maintained in the lung tissue immediately after drowning. Particularly, it was possible to clearly distinguish the drowning water temperature between bathtub drowning model and winter river drowning model. Despite the inhaled water temperature being unknown, the change of T1 relaxation time may be useful when distinguishing between cold and hot water aspirations. This investigation provides baseline values of drowning lung tissues. Moreover, the T2 relaxation time could reflect the characteristics of a drowning lung tissue. These results may be useful for the qualitative assessments of drowning lung and can serve as a basis when imaging a human body in forensic practice.

Declaration of Competing Interest

None.

Acknowledgements

This study was supported by Laboratory Animal Facilities in The Jikei University School of Medicine, Tokyo, Japan. We would like to thank Prof. Kanuka Hirotaka and all of the laboratory animal facilities. The authors have no conflicts of interest. We would like to thank Enago (www.enago.jp) for the English language review.

References

[1] N. Beckmann, B. Tigani, L. Mazzoni, J.R. Fozard, MRI of lung parenchyma in rats and mice using a gradient-echo sequence, NMR Biomed. 14 (5) (2001) 297–306, https://doi.org/10.1002/(ISSN)1099-149210.1002/nbm.v14:510.1002/nbm.706.

[2] L.E. Olsson, P.D. Hockings, V. Schöpf, In vivo measurements of T2 relaxation time of mouse lungs during inspiration and expiration, PLoS One. 11 (12) (2016) e0166879, https://doi.org/10.1371/journal.pone.0166879.

[3] A.G. Cutillo, P.H. Chan, D.C. Ailion, S. Watanabe, K.H. Albertine, C.H. Durney, C. B. Hansen, G. Laicher, R.F. Scheel, A.H. Morris, Effects of endotoxin lung injury on NMR T2relaxation, Magn Reson Med. 39 (2) (1998) 190–197, https://doi.org/10.1002/mrm.1910390205.

[4] D.F. Alamidi, S.S.I. Kindvall, P.L. Hubbard Cristinacce, D.M. McGrath, S.S. Young, J.H. Naish, J.C. Waterton, P. Wollmer, S. Diaz, M. Olsson, P.D. Hockings, K. M. Lagerstrand, G.J.M. Parker, L.E. Olsson, A. Larcombe, T1 Relaxation time in lungs of asymptomatic smokers, PLoS One 11 (3) (2016) e0149760, https://doi.org/10.1371/journal.pone.0149760.

[5] M.T.A. Buzan, A. Wetscherek, C.P. Heussel, M. Kreuter, F.J. Herth, A. Warth, H.-U. Kauczor, C.M. Pop, J. Dinkel, G. Zissel, Texture analysis using proton density and T2 relaxation in patients with histological usual interstitial pneumonia (UIP) or nonspecific interstitial pneumonia (NSIP), PLoS One 12 (5) (2017) e0177689, https://doi.org/10.1371/journal.pone.0177689.

[6] N. Bloembergen, E.M. Purcell, R.V. Pound, Relaxation effects in nuclear magnetic resonance absorption, Phys. Rev. 73 (7) (1948) 679–712, https://doi.org/10.1103/PhysRev.73.679.

[7] C.J. Lewa, Z. Majewska, Temperature relationships of proton spin-lattice relaxation time T1 in biological tissues, Bull. Cancer 67 (5) (1980) 525–530.

[8] T.R. Nelson, S.M. Tung, Temperature dependence of proton relaxation times in vitro, Magn. Reason Imaging. 5 (3) (1987) 189–199, https://doi.org/10.1016/0730-725x(87)90020-8.

[9] P.A. Bottomley, T.H. Foster, R.E. Argersinger, L.M. Pfeifer, A review of normal tissue hydrogen NMR relaxation times and relaxation mechanisms from 1–100 MHz: dependence on tissue type, NMR frequency, temperature, species, excision, and age, Med. Phys. 11 (4) (1984) 425–448, https://doi.org/10.1118/1.595535.

[10] C. Birkl, C. Langkammer, J. Haybaeck, C. Ernst, R. Stollberger, F. Fazekas, S. Ropele, Temperature-induced changes of magnetic resonance relaxation times in the human brain: a postmortem study, Magn. Reason. Med. 71 (4) (2014) 1575–1580, https://doi.org/10.1002/mrm.24799.

[11] S. Shiotani, T. Kobayashi, H. Hayakawa, K. Homma, H. Sakahara, Hepatic relaxation times from postmortem MR imaging of adult humans, Magn. Reason. Med. Sci. 15 (3) (2016) 281–287, https://doi.org/10.2463/mrms.mp.2015-0086.

[12] S.S.I. Kindvall, S. Diaz, J. Svensson, P. Wollmer, D. Slusarczyk, L.E. Olsson, Influence of age and sex on the longitudinal relaxation time, T1, of the lung in healthy never-smokers, J. Magn. Reason. Imaging 43 (5) (2016) 1250–1257, https://doi.org/10.1002/jmri.25085.

[13] O. Dietrich, T. Gaass, M.F. Reiser, T1 relaxation time constants, influence of oxygen, and the oxygen transfer function of the human lung at 1.5 T—a meta-analysis, Eur. J. Radiol. 86 (2017) 252–260, https://doi.org/10.1016/j.ejrad.2016.11.027.

[14] F. Satoh, M. Osawa, I. Hasegawa, Y. Seto, A. Tsuboi, Dead in hot bathtub phenomenon: accidental drowning or natural disease? Am. J. Forensic Med. Pathol. 34 (2) (2013) 164–168, https://doi.org/10.1097/PAF.0b013e31828d68c7.

[15] Y. Kanawaku, T. Tanifuji, Y. Ohno, Association between sudden unexpected deaths in bathtubs and ambient temperature among elderly Japanese adults: a time-series regression study, Leg. Med. 2019 (36) (2018) 21–27, https://doi.org/10.1016/j.legalmed.2018.09.021.

[16] W.H. Hsieh, C.H. Wang, T.H. Lu, Drowning mortality by intent: a population-based cross-sectional study of 32 OECD countries, 2012–2014, BMJ Open 8 (7) (2018) 1–6, https://doi.org/10.1136/bmjopen-2018-021501.

[17] T. Hayashi, Y. Ishida, S. Mizunuma, A. Kimura, T. Kondo, Differential diagnosis between freshwater drowning and saltwater drowning based on intrapulmonary aquaporin-5 expression, Int. J. Legal. Med. 123 (1) (2009) 7–13, https://doi.org/10.1007/s00414-008-0235-5.

[18] H. Maeda, B.-L. Zhu, T. Ishikawa, L.i. Quan, T. Michiue, Y. Bessho, S. Okazaki, Y. Kamikodai, K. Tsuda, A. Komatsu, Y. Azuma, Analysis of postmortem biochemical findings with regard to the lung weight in drowning, Leg. Med. 11 (2009) S269–S272, https://doi.org/10.1016/j.legalmed.2009.01.029.

[19] D. Yajima, G.o. Inokuchi, Y. Makino, A. Motomura, F. Chiba, S. Torimitsu, R. Yamaguchi, Y. Hoshioka, D. Malakienė, R. Raudys, H. Iwase, Diagnosis of drowning by summation of sodium, potassium, and chloride ion levels in sphenoidal sinus fluid: differentiating between freshwater and seawater drowning and its application to brackish water and bathtub deaths, Forensic Sci. Int. 284 (2018) 219–225, https://doi.org/10.1016/j.forsciint.2018.01.013.

[20] P.S. Vander, E. De Letter, M. Piette, G. Van Parys, J.W. Casselman, K. Verstraete, Post-mortem evaluation of drowning with whole body CT, Forensic Sci. Int. 249 (2015) 35–41, https://doi.org/10.1016/j.forsciint.2015.01.008.

[21] S. Mishima, H. Suzuki, T. Fukunaga, Y. Nishitani, Postmortem computed tomography findings in cases of bath-related death: applicability and limitation in forensic practice, Forensic Sci. Int. 282 (2018) 195–203, https://doi.org/10.1016/j.forsciint.2017.11.030.

[22] T. Miyazato, T. Ishikawa, T. Michiue, H. Maeda, Molecular pathology of pulmonary surfactants and cytokines in drowning compared with other asphyxiation and fatal hypothermia, Int. J. Legal Med. 126 (4) (2012) 581–587, https://doi.org/10.1007/s00414-012-0698-2.

[23] J.M. Wild, H. Marshall, M. Bock, L.R. Schad, P.M. Jakob, M. Puderbach, F. Molinari, E.J.R. Van Beek, J. Biederer, MRI of the lung (1/3): methods, Insights Imaging. 3 (4) (2012) 345–353, https://doi.org/10.1007/s13244-012-0176-x.
[24] S. Kawai, Y. Takagi, S. Kaneko, T. Kurosawa, Effect of three types of mixed anesthetic agents alternate to ketamine in mice, Exp. Anim. 60 (5) (2011) 481–487, https://doi.org/10.1538/expanim.60.481.
[25] J.-J. Yuan, X.-T. Zhang, Y.-T. Bao, X.-J. Chen, Y.-Z. Shu, J.-L. Chen, W. Chen, B. Du, Q.-F. Pang, Heme oxygenase-1 participates in the resolution of seawater drowning-induced acute respiratory distress syndrome, Respir. Physiol. Neurobiol. 247 (2018) 12–19, https://doi.org/10.1016/j.resp.2017.08.016.
[26] F. Aeffner, B. Bolon, I.C. Davis, Mouse models of acute respiratory distress syndrome, Toxicol. Pathol. 43 (8) (2015) 1074–1092, https://doi.org/10.1177/0192623315598399.
[27] A. Christe, E. Aghayev, C. Jackowski, M.J. Thali, P. Vock, Drowning - post-mortem imaging findings by computed tomography, Eur. Radiol. 18 (2) (2008) 283–290, https://doi.org/10.1007/s00330-007-0745-4.
[28] I.R. Young, J.W. Hand, A. Oatridge, M.V. Prior, Modeling and observation of temperature changes in vivo using MRI, Magn. Reason Med. 32 (3) (1994) 358–369, https://doi.org/10.1002/mrm.1910320311.
[29] M. Estilaei, A. MacKay, K. Whittall, J. Mayo, In vitro measurements of water content and T2relaxation times in lung using a clinical MRI scanner, J. Magn. Reason Imaging 9 (5) (1999) 699–703, https://doi.org/10.1002/(SICI)1522-2586(199905)9:5<699::AID-JMRI12>3.0.CO;2-H.
[30] H. Hyodoh, J. Shimizu, M. Rokukawa, S. Okazaki, K. Mizuo, S. Watanabe, Postmortem computed tomography findings in the thorax - experimental evaluation, Leg. Med. 2016 (19) (2015) 96–100, https://doi.org/10.1016/j.legalmed.2015.07.015.
[31] S. Thayyil, N.J. Sebire, L.S. Chitty, et al., Post mortem magnetic resonance imaging in the fetus, infant and child: a comparative study with conventional autopsy (MaRIAS Protocol), BMC Pediatr. 11 (1) (2011), https://doi.org/10.1186/1471-2431-11-120.
[32] S. Thayyil, N.J. Sebire, L.S. Chitty, et al., Post-mortem MRI versus conventional autopsy in fetuses and children: a prospective validation study, Lancet 382 (9888) (2013) 223–233, https://doi.org/10.1016/S0140-6736(13)60134-8.
[33] S. Thayyil, M. Chandrasekaran, L.S. Chitty, et al., Diagnostic accuracy of post-mortem magnetic resonance imaging in fetuses, children and adults: a systematic review, Eur. J. Radiol. 75 (1) (2010) e142–e148, https://doi.org/10.1016/j.ejrad.2009.10.007.
[34] O.J. Arthurs, A. Guy, S. Thayyil, et al., Comparison of diagnostic performance for perinatal and paediatric post-mortem imaging: CT versus MRI, Eur. Radiol. 26 (7) (2016) 2327–2336, https://doi.org/10.1007/s00330-015-4057-9.
[35] P. Montaldo, S. Addison, V. Oliveira, et al., Quantification of maceration changes using post mortem MRI in fetuses, BMC Med. Imaging 16 (1) (2016), https://doi.org/10.1186/s12880-016-0137-9.